ENGINEERING RESEARCH JOURNAL (ERJ)

Vol. 1, No. 51 Jan 2022, pp.20-28

Journal Homepage: http://erj.bu.edu.eg

An experimental investigation of the Evacuated Tube solar collector in conjunction with a latent heat storage tank

Rashed M.Almari, Mohamed A. Abdelrahman, Mohamed A. Moawad.

Department of Mechanical Engineering, Benha University, Egypt

Abstract

A latent heat storage tank with a helical coil heat exchanger was developed, built, connected to an evacuated tube solar collector, and tested in this study. 25 kg of paraffin wax was used as phase change material (PCM) in the storage tank. During the charging (melting) process, the storage system was evaluated with varied mass flow rates of hot water as a heat transfer medium (5, 8, 9, 10.5 and 13 L/min). The system was also tested with a constant mass flow rate of domestic water during the discharging cycle (solidification). The results also showed that increasing the flow rate from 5 L/min to 13 L/min reduced the charging time from 218 min to 157 min and increased the system's overall efficiency from 28.4 % to 40.5 %.

Keywords: solar collector, Phase change material, Energy storage, solar radiation.

Nomenclature:

Symbol	Description	Symbol	Description
A	solar collector area (m2)	m_{PCM}	mass of the PCM (kg)
C_W	specific heat of the water (J/kg °C)	m_w	mass of water in domestic reservoir (kg)
C_{PCM}	specific heat of the PCM (J/kg °C)	PW	paraffin wax
ETSWH	Evacuated Tube solar water heater	PCM	phase change material
HTF	heat transfer fluid	Q_{in}	the energy inlet to of the ETSWH (kJ)
HP	horse power	Q_w	the stored energy in water (kJ)
I	Global solar radiation intensity (W/m^2)	Q_{PCM}	the stored energy in PCM (kJ)
l	Litter	T_{am}	ambient temperature (°C)
LH	Latent heat of the wax (kJ/kg).	T_{w_h}	Hot water temperature at the end of discharge cycle (°C)
Greek Symbols		T_{w_c}	Cold water temperature at the start of discharge cycle (°C)
$\eta_{storage}$	Storage efficiency	T	temperature, (°C)
η_{useful}	useful efficiency heating domestic water	ΔT	temperature difference (°C)
$\eta_{overall}$	System overall efficiency	T_{PCM}	Paraffin wax (temperature , (°C)
ω	Uncertainty	t	Cycle time (s)

1. Introduction

Solar thermal energy is regarded as the most promising renewable energy source owing to its cleanliness, sustainability, and availability in many regions of the world, as the Sun emits energy at a rate of 3.8×10^{23} kW per second, of which roughly 1.08×10^{14} kW is reaches the surface of the earth[1][2].Although if only 0.1 %t of this energy could be transformed at a 10% efficiency, it really would be 4 times the global production generating capacity of about 3000 GW. To put it differently, the total yearly solar radiation incidence on the earth is much more than 7500 times the total worldwide annual energy usage [2]. There is a lot of potential for using accessible solar energy for thermal applications like cooking, water heating, crop drying, air-conditioning, power plants and so on.

The solar collector is the most important part of any solar thermal application. It collects solar energy, transforms it to heat, and transmits the heat to raise the enthalpy of working fluid (often air, water, or oil) that flows through it [3]. There are several types of solar collectors used in water heating (flat plate, evacuated tube, parabolic trough and parabolic dish). The type of collector to be used is determined by the output temperature requirement for a specific application.

During the period of sunshine, the solar collector works efficiently for only a few hours. Unfortunately, thermal loads rise throughout the night, and because solar energy is intermittent, it is critical to provide a storage system to mitigate the mismatch problem [4]. Energy storage improves system reliability and performance while reducing supply and demand mismatch [5].It saves fuel and makes systems more economical by reducing energy waste and capital costs. The use of phase change materials (PCM) as a latent heat storage material is a promising technique for thermal energy storage and a potential solution to the previously noted mismatch problem [6].

PCMs are materials that can store and release energy while melting and solidifying at a certain temperature. The heat of fusion for these substances should be high in order to store a large quantity of energy and discharge it when needed. PCMs are divided into three types: organic, inorganic, and eutectic. Organic materials (128–200 kJ/kg) have approximately halved the latent heat storage capacity of inorganic materials (250–400 kJ/kg)[7]. In the same melting point range, organic PCM offers certain benefits over inorganic PCM since it is chemically stable and compatible with metal, as well as being relatively cheap [8]. As a result, paraffin wax is an appropriate material for the current work.

Paraffin wax is found in coal, natural gas, and petroleum [9]. It is distinguished by having distinct and stable thermophysical properties for energy storage [10]. Because paraffin wax's thermal properties do not deteriorate even after 1000-2000 melt/freeze cycles, it is safe, non-reactive, and compatible with all metal containers [11]

Zakir and Zulfiqar [12] have proposed a unique concept of a latent heat storage system combined with flat plate solar collector . They employed paraffin wax as PCM medium inside a shell and tube heat exchanger with longitudinal fins and utilized water as a working fluid. They discovered that the proposed system can store around 14.36 MJ of solar energy in 3.12 hours when charged at inlet temperature of 62 °C and water volume flow rate of 1.5 L/min. Furthermore, numerous storage units may be connected in parallel to meet any household or business energy need.

Following a review of the prior literature, it was found that there are numerous interpretations of studying the performance of thermal storage for solar collectors, improving it, and increasing its economic feasibility. The research focused on a variety of factors, including the physical properties of the storage material and the additives that improve its properties, the type and area of the solar collector, the type and flow rate of the heat transfer fluid, the design of the heat exchanger, and others.

As a result, the current research is important in that it aims to design and implement a simple and inexpensive solar thermal storage system, the components of which are readily available in the local market and consist of a simple helical coil heat exchanger and inexpensive paraffin wax.

This is accomplished by connecting the evacuated tube solar water heater (ETSWH) to the PCM tank and analyzing the integrated thermal storage performance (charging and discharging) of the system with varying heat transfer fluid flow rates (5–13 L/min) during the charging process and a fixed flow rate of 18 L/min during discharging process.

2. Experimental set up

This section will go over the current system characterization, experimental setup, measurement instrumentation and specifications in detail. Because the current study's goal is to evaluate the performance of a solar energy storage system, an evacuated tube solar water heater (ETSWH) with a collector area of 1.86 $m^2$and tilted by 42° from horizontal was evaluated. The experiment is made up of two circuits, as depicted inFigure 1.

The first is a charging circuit in which the solar energy is stored in a tank filled with Paraffin wax as PCM, and the hot water produced by the solar heater is pumped by a 1/2 HP pump to a helical coil heat exchanger with a height of 40 cm and made of 1/2 inch copper tubes with 14 rings, each with a diameter of 15 cm. The coil is housed within a stainless steel tank with a diameter of 30 cm, a thickness of 2 mm, and a height of 50 cm. In all tests, purified water was utilized as a medium for heat transfer HTF across the circuit, and the water flow rate was regulated by a needle valve after the pump and a digital turbine flow meter read via Arduino code.

To guarantee that the pipe was entirely filled with water and that there were no air pocketswithin the solar collector and heat exchanger, an air vent valve was employed. The system was tested in summer 2021, with the HTF flow rate varying between 5, 8, 9, 10.5, and 13 L/min. Each flow rate's pressure drop via the helical coil was also monitored using a digital manometer, as shown in Figure 2.

The second circuit is a discharge circuit, in which the energy stored in the wax is utilized by solidifying the wax by passing cold water through another helical coil heat exchanger located within the wax tank, which has the same construction as the coil used in the charging circuit. A 75-liter domestic water tank is utilized, and the water is pumped by a 1/2 HP pump into the PCM tank, where it heats up, and then returned to the water tank. The flow rate of cold water in this circuit is kept constant at 18 L/min and is regulated by another digital turbine flow-meter programmed with Arduino code.At the end of the experiment, the vent port in the PCM tank is opened to the atmosphere to ensure that the wax has completely solidified before starting the next experiment the following day.

Because of its high latent heat and long-term dependability, paraffin wax with a melting temperature of 60℃ was chosen to function as PCM. Table 1 shows the physical characteristics of the PW utilized in this investigation. The charging circuit was activated at 9:00 a.m. until the minimum PCM temperature within the storage tank reached 60℃, ensuring that the whole PCM inside the tank was melted. After ensuring that all of the wax has melted, the charging pump is switched off andthe ETSWH is covered, followed by the discharge pump, which extracts heat from the melted wax and heats the domestic water tank. When the temperature of the water entering and exiting the tank becomes stable and equal to the temperature of the solidified wax, the discharging circuit is turned off. The following 8 thermocouples of type K were distributed: 5 inside the PCM tank (bottom-top-middle-left-right), then the average value was determined and recorded as T_{PCM}, one upon entering the heat exchanger, one upon exiting the exchanger, and one upon the atmosphere to measure wax, water, and ambient temperatures during charge and discharge circuits, respectively. Temperatures were read and recorded every minute using a PICO thermocouple data logger. TES-1333R Data logging solar power meter was installed in plane normal to the ETSWH to record the global solar radiation.

Table 1: Paraffin wax physical properties.[4][13][14]

Melting point ℃	Liquid/Solid Density kg/m^3	Liquid/Solid Specific heat kJ/kg K	Latent heat kJ/kg	Liquid/Solid Thermal conductivity W/m K
58.7 - 60	840 / 900	2.2 / 1.9	190	0.22/0.24

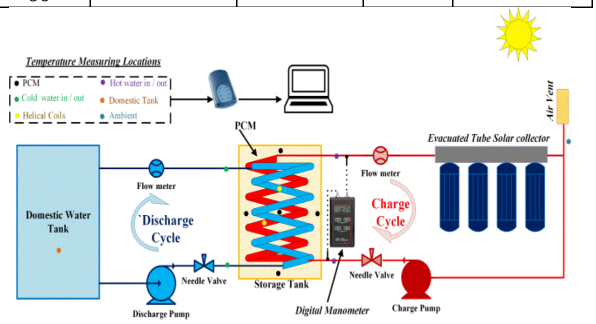

Fig 1: a graphical depiction of the current experimental setup.

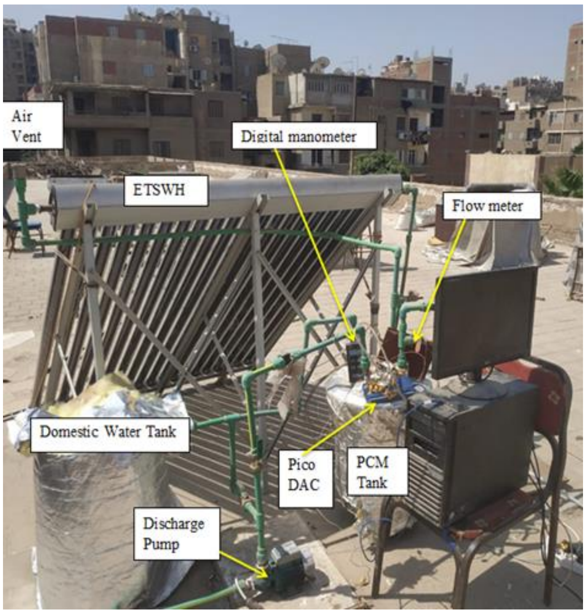

Fig 2: a picture of ETSWH combined with PCM and a domestic water storage tank.

3. Data Reduction

Microsoft Excel spreadsheets have been created to process the experimental data for storage energy, storage efficiency, and total efficiency. This section contains the equations for the system's assessment criteria.

During the charging period, the energy source of ETSWH may be estimated as follows:

$$Q_{in} = \int_0^t I\,A\,dt \quad (1)$$

Where I denote incoming global solar radiation (W/m^2), A is solar collector area as given by manufacturer(m^2), and t denotes the duration of charging cycle.

The energy stored in the paraffin wax PCM (Q_{pcm}) is given by[15];

$$Q_{pcm} = m_{PCM} C_{PCM} \Delta T + LH\, m_{PCM} \quad (2)$$

Where $m_{PCM}$is the wax mass (kg) is, C_{PCM} is the wax specific heat (J/kg°C), ΔT is the temperature difference of the wax (°C) and LH is the wax latent heat (J/kg).

The storage efficiency ($\eta_{storage}$) during the charging period can be written as [15];

$$\eta_{storage} = \frac{Q_{PCM}}{Q_{in}} \quad (3)$$

The useful storage energy in water (Q_w) is provided by [13]

$$Q_w = m_w C_w (T_{w\_h} - T_{w\_c}) \quad (4)$$

Where m_w represents the amount of water in the domestic tank (kg), C_w represents the specific heat of water (J/kg °C), T_{w_h}represents the hot water temperature at the end of discharge cycle (°C), and T_{w_c} represents the cold water temperature at the end of discharge cycle (°C)

The useful efficiency in heating the domestic water can be written as [16],

$$\eta_{useful} = \frac{Q_w}{Q_{pcm}} \quad (5)$$

The system overall efficiency can be calculated as:

$$\eta_{overall} = \eta_{usefull} \times \eta_{storage} \quad (6)$$

3.1. Experimental errors and uncertainties

When conducting experimental work, one of the most crucial elements to consider is uncertainty analysis. This study is primarily dependent on the accuracy of the instruments employed.

$$if\ y = f(x_1, x_2, x_3, \dots \dots \dots, x_n)$$

The root sum square combination of the impacts of each individual independent parameter (x) on the dependent parameter (y), as presented by Kline and McClintock [17], is used in this work to calculate the uncertainty in all variables as;

$$\omega_y = \left[\left(\frac{\partial y}{\partial x_1}\omega_{x_1}\right)^2 + \left(\frac{\partial y}{\partial x_2}\omega_{x_2}\right)^2 + \dots + \left(\frac{\partial y}{\partial x_n}\omega_{x_n}\right)^2\right]^{0.5} \quad (7)$$

From equation (1) the uncertainty of input solar energy can be calculated as:

$$\omega_{Q_{in}} = \left[\left(\frac{\partial Q_{in}}{\partial I}\omega_I\right)^2 + \left(\frac{\partial Q_{in}}{\partial A}\omega_A\right)^2 + \left(\frac{\partial Q_{in}}{\partial t}\omega_t\right)^2\right]^{0.5} \quad (8)$$

By using the measuring devices errors in Table 2 , The relative uncertainty of input solar energy can be calculated as:

$$\therefore \frac{\omega_{Q_{in}}}{Q_{in}} = \left[\left(\frac{\omega_I}{I}\right)^2 + \left(\frac{\omega_A}{A}\right)^2 + \left(\frac{\omega_t}{t}\right)^2\right]^{0.5} = [(0.5)^2 + (0.25)^2 + (0.166)^2]^{0.5} = 0.583\ \% \quad (9)$$

From equation (2) the relative uncertainty of the stored energy in PCM can be calculated as:

$$\therefore \frac{\omega_{Q_{PCM}}}{Q_{PCM}} = \left[\left(\frac{\omega_{m_{PCM}}}{m_{PCM}}\right)^2 + \left(\frac{\omega_{T_{PCM,final}}}{T_{PCM,final}}\right)^2 + \left(\frac{\omega_{T_{PCM,intial}}}{T_{PCM,intial}}\right)^2\right]^{0.5} = [(0.05)^2 + (0.18)^2 + (0.18)^2]^{0.5} = 0.262\ \% \quad (10)$$

From equation (3) the relative uncertainty of the storage efficiency can be calculated as:

$$\therefore \frac{\omega_{\eta_{storage}}}{\eta_{storage}} = \left[\left(\frac{\omega_{Q_{PCM}}}{Q_{PCM}}\right)^2 + \left(\frac{\omega_{Q_{in}}}{Q_{in}}\right)^2\right]^{0.5} = [(0.583)^2 + (0.262)^2]^{0.5} = 0.593\ \% \quad (11)$$

From equation (4) the relative uncertainty of the useful storage energy in water can be calculated as:

$$\therefore \frac{\omega_{Q_w}}{Q_w} = \left[\left(\frac{\omega_{m_{w^\cdot}}}{m_{w^\cdot}}\right)^2 + \left(\frac{\omega_{T_{w_h}}}{T_{w_h}}\right)^2 + \left(\frac{\omega_{T_{w_c}}}{T_{w_c}}\right)^2\right]^{0.5} = [(0.666)^2 + (0.18)^2 + (0.18)^2]^{0.5} = 0.7145\ \% \quad (12)$$

From equation (5) the relative uncertainty of useful the efficiency can be calculated as:

$$\therefore \frac{\omega_{\eta_{useful}}}{\eta_{useful}} = \left[\left(\frac{\omega_{Q_w}}{Q_w}\right)^2 + \left(\frac{\omega_{Q_{PCM}}}{Q_{PCM}}\right)^2\right]^{0.5} = [(0.7145)^2 + (0.262)^2]^{0.5} = 0.761\ \% \quad (13)$$

From equation (6) the relative uncertainty of the overall efficiency can be calculated as:

$$\therefore \frac{\omega_{\eta_{overall}}}{\eta_{overall}} = \left[\left(\frac{\omega_{\eta_{useful}}}{\eta_{useful}}\right)^2 + \left(\frac{\omega_{\eta_{storage}}}{\eta_{storage}}\right)^2\right]^{0.5} = [(0.761)^2 + (0.593)^2]^{0.5} = 0.965\ \% \quad (14)$$

Table 2: Measuring devices specifications.

Thermocouples	Type Accuracy Range	K-Type ± 0.5 ℃ 0 – 275 ℃
Data Acquisition system	Type Accuracy Range	Pico TC- 08 ±0.2 % - 270 to 1370 ℃
Solar power meter	Type Accuracy Range	TES 1333R ±10 W/m2 0–2000 W/m2
Digital Anemometer	Model Velocity range – accuracy Temperature range	GT8907 (0–45) m/s – ±3% (0–45) ◦C – ±1 ◦C
Turbine flow meter	Type Accuracy Range	G12 ± 0.2 L/min (1–30) L/min
Digital Weight Scale	Accuracy Range	± 1 gram 0-2000 gram
Clock	Accuracy Range	± 20 second 0-218 minutes

4. Results and Discussion

The ETSWH was evaluated in this study with paraffin wax as thermal energy storage materials. During the period (30/8/2021–4/9/2021), the ETSWH was tested at various HTF flow rates (5–13 L/min).

Experiments are carried out in two stages: the first is the charging stage, in which solar energy is stored in the wax tank as molten wax, and the second is the extraction of energy from the molten wax to heat the domestic water.

4.1. Charging circuit

Figure 3depicts the solar radiation and ambient temperature measurements taken on all test days. It is apparent that the greatest levels of global solar radiation observed throughout the trials ranged from 864 to 905 W/m^2, with an average ranging from 755 to 767 W/m^2. While the average ambient temperature observed during the trials ranged from 37.5 to 41 ˚C.

Five temperatures distributed in the wax inside the tank are recorded, and the average temperature is taken as the wax temperature. The measurements begin at 9 a.m. and continue until the lowest temperature inside the tank reaches the melting point (60 ˚C), ensuring that all of the wax has melted. Figure 4 depicts the variation in average wax temperature during the charging process at various HTF volume flow rates.

From the figure, it is clearly that the temperature of the wax gradually increases with the increase in solar radiation, as the wax passes through three stages, the first being the sensible heating stage, in which the temperature of the solid wax rises until it reaches its melting temperature due to the specific heat of the wax, after that with the increase in radiation, The latent heat of the wax causes it to melt and transform into a liquid state at almost constant temperature , which is the second stage.The temperature of the molten wax then gradually rises due to the perceived heat as the radiation increases until the end of the charging stage, at which point the charge pump is turned off, the solar collector is covered, the discharging pump is activated, and the discharge cycle begins.

The influence of changing the water volume flow rate on the charging process rates is depicted in Figure 5. The charging time is the amount of time required to ensure that the wax inside the tank has completely melted. It is clear that increasing the flow rate from 5 to 13 L/min increases the rate of heat transfer from hot water to wax, accelerating the melting process and reducing charging time from 218 minutes to 157 minutes.

based on average PCM temperature , Figure 6 depicts the accumulated stored energy in the PCM during the charging time at the highest flow rate of 13 L/min. is apparent that the wax is heated by sensible heat for 90 min until it reaches the commencement of melting at around (the average wax temperature equal 58.5℃). The wax then takes around 20 minutes to completely melt owing to latent heat, and the stored energy during that time is quite considerable due to the high value of latent heat (LH) compared to the low specific heat value (C_p), and the melting period varies depending on the flow rate. After melting, the average temperature of the wax starts to rise owing to sensible heat until the charging time is completed.

The storage efficiency during the charging period can be calculated as a percentage of the total useful energy stored in the PCM divided by the accumulated solar energy incident during the charging period, as shown in Figure 7, where it is clear that the storage efficiency increases with the increase in the water flow rate, as it recorded 31.5 % at the flow rate of 5 L/min and increased to 50 % at the flow rate of 13 L/min.

Although the heat transfer rate and storage efficiency increase with the increase in the water flow rate, on the contrary, the friction in the heat exchanger also increases and the pressure difference increases, resulting in an increase in pumping power.A digital manometer was used to measure the pressure drop for each volume flow rate, and the results are shown in Figure 8.

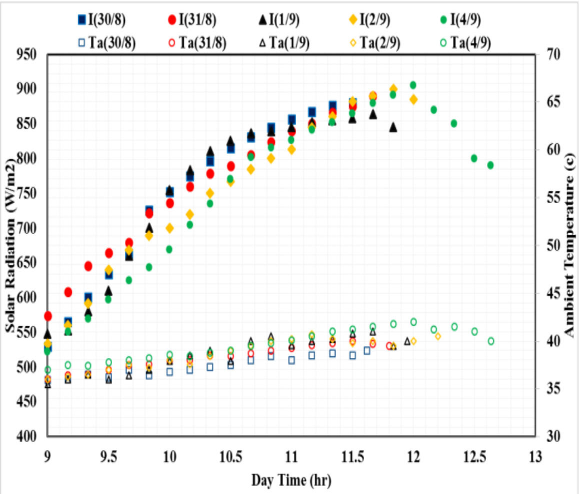

Fig 3: Variation in solar radiation and ambient temperature during charge process on allTest days.

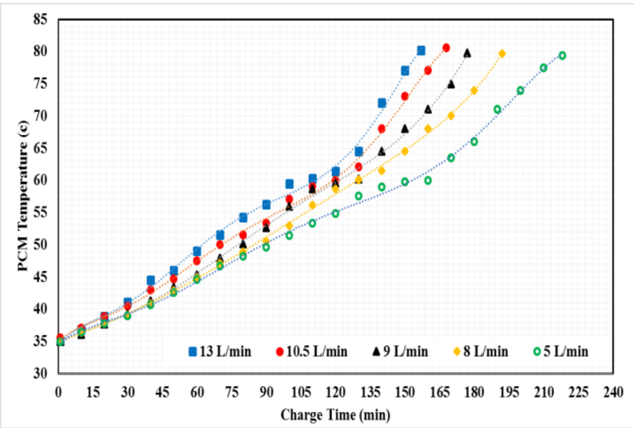

Fig 4: The variation in PCM temperature throughout the charging process at various HTF volume flow rates.

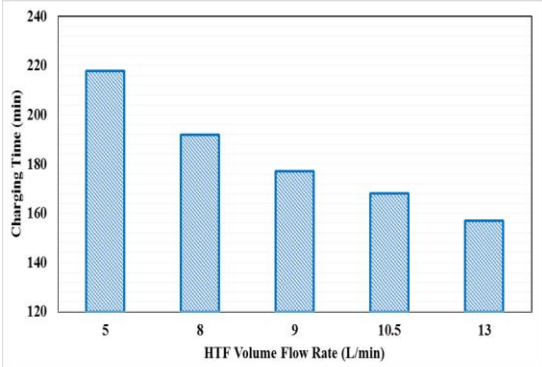

Fig 5: Effect of changing the HTF volume flow rate on the charging time.

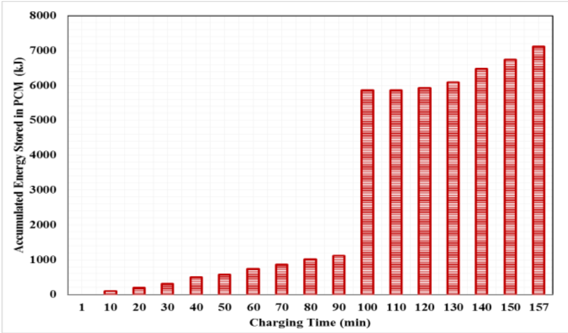

Fig 6: The accumulated stored energy in the PCM during the charging process at 13 L/min.

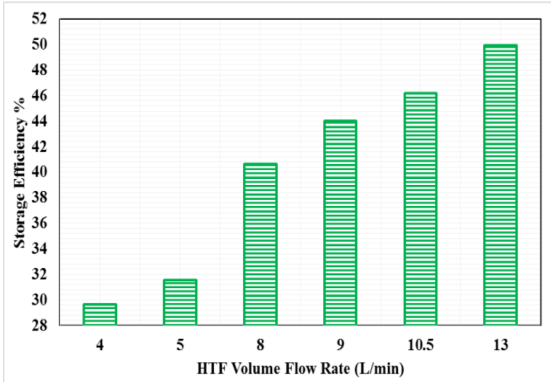

Fig 7: The variation of storage efficiency at different HTF volume flow rate.

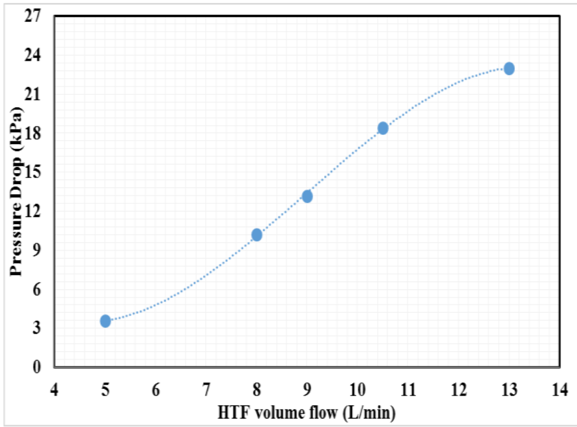

Fig 8: The variation of pressure drop at different HTF volume flow rate.

4.2. Discharging circuit

After ensuring that the wax has completely melted during the charging stage, the charging pump is turned off and the solar collector is covered, and the discharge pump is turned on to extract the energy stored in the wax by pumping cold water from a 75-liter tank at a constant flow rate of 18 L/min as the discharging pump's maximum flow rate, while the water flow rate varies during the charging stage.

Figure 9 displays the PCM temperature as recorded on a day of 30/8/2021whereas the cycle was running at its optimum charging mass flow rate of 13 L/min. The PCM temperature rises with time, simulating solar radiation, reaching a peak of 80.1 °C after 157 minutes (11:37 A.M). At that moment, the charging pump is turned off, the discharging pump is turned on, and domestic water is pumped in the PCM tank to gain heat from melted wax. As a consequence, the PCM temperature progressively lowers while the temperature of the water within the domestic water tank gradually increases until it reaches a stable state at 52.3 °C, at which point the pump is turned off until the heat is dissipated from the water tank due to stirring.

The useful efficiency during the discharging period can be calculated as a percentage of the amount of heat used in heating water divided by the accumulated energy stored in PCM during the charging period, as shown in Figure 10, The figure clearly shows that the useful efficiency increases significantly at the start of the discharge process, where there is a large difference between the temperatures of wax and domestic water, but with time, the two temperatures converge and the efficiency increases slightly until it is almost constant at the end of the cycle, and the accumulative useful efficiency reached up to 81%.

When evaluating the entire system while accounting for both the charging and discharging periods, the overall efficiency of the system can be calculated by multiplying the storage efficiency by the useful efficiency, and it is clear that the overall efficiency increases as the HTF flow rate increases, as shown in Figure 11.

It is also evident that the greatest efficiency attained at a flow rate of 13 L/min is 40.5%, which is a low figure. This is most likely owing to the presence of several regions inside the PCM tank that do not have direct contact between the heat exchanger coils and the PCM due to the design of the helical coil without fins, and therefore the melting process is delayed in those areas. This decrease is also probable owing to paraffin wax's poor coefficient of heat conductivity, which is one of its main disadvantages when employed in thermal storage [4][18].

Table 3 summarizes the experimental data obtained from the current study in comparison to three different published results.

The table shows that each solar thermal energy storage system has characteristics and features that affect system performance and differ from one system to another. Among these characteristics is the type of storage material and its improved additives, the type of solar collector and its surface area, HTF flow rate, heat exchanger design, and so on.

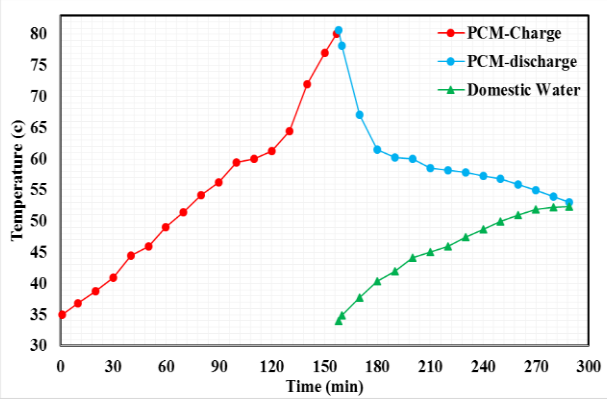

Fig 9: The temperature fluctuation of the PCM during charge and discharge at a maximum mass flow rate of 13 L/min.

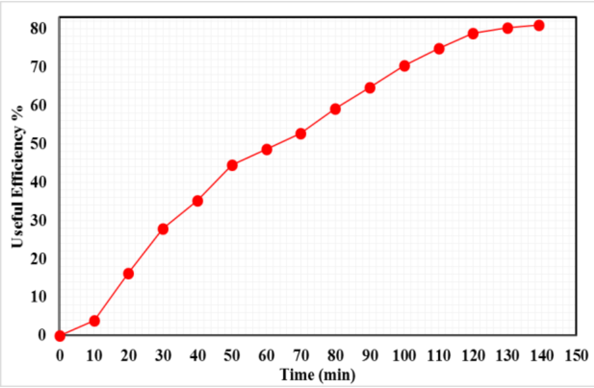

Fig 10: variation of useful efficiency during discharge at a maximum mass flow rate of 13 L/min.

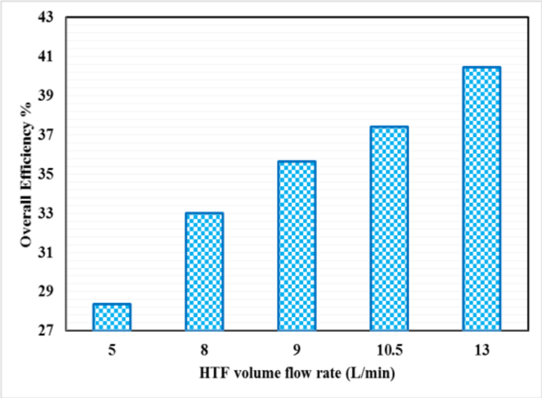

Fig 11: system overall efficiency variation at different HTF mass flow rate.

Table 3:A comparison of the current storage system with three previous published systems.

item	Current work	[4]	[19]	[13]
Solar collector area (m^2) / type	1.86 m^2 Evacuated tube	2.37 m^2 Flat plate	-	1m^2 Flat plate
Storage type	Paraffin wax (PW)	PW	PW - graphite compound	PW– nano Cu particles
Heat exchanger design	Helical coil	Shell and finned tube	Helical coil	-
PCM mass (kg)	25	50	3	28 & 2.8 g nano
Water volume (Litter)	75	110	150	60
Max. water temperature (°C)	52.4	57.3	-	59.1
Max. PCM temperature (°C)	81	59.9	67	-
Optimum HTF flow rate (l/min)	13	9.6	-	0.5
Daily efficiency %	40.5	43	74	68.8

5. Conclusions

In this study, the ETSWH was investigated in summer 2021 with paraffin wax as thermal energy storage materials. Five different HTF volume flow rates (5, 8, 9, 10.5 and 13 L/min) during the charging cycles were experimentally studied, with a domestic water flow rate of 18 L/min fixed during the discharge cycle, and the following conclusions were reached:

1. Increasing the flow rate from 5 L/min to 13 L/min during the charging cycle reduces the charging time from 218 minutes to 157 minutes, resulting in a faster melting and charging process.
2. The ETSWH performed better in conjunction with the PCM tank at the maximum HTF volume flow rate of 13 L/min, with a storage efficiency of 50%.
3. The useful efficiency during the discharging process time achieved 81 % at the HTF volume flow rate of 13 L/min, where the water temperature climbed by around 18.4 °c, rising from 34 °c to 52.4 °c.
4. The maximum value of overall efficiency obtained is 40.5 %, which is a low value; to improve this value, we recommend using a heat exchanger with fins to increase the contact surfaces between the exchanger and the PCM, as well as adding Nano particle materials to the PCM to improve thermal conductivity and thus storage efficiency

References

[1] N. L. Panwar, S. C. Kaushik, and S. Kothari, "Role of renewable energy sources in environmental protection: A review," *Renew. Sustain. Energy Rev.*, vol. 15, no. 3, pp. 1513–1524, 2011, doi: 10.1016/j.rser.2010.11.037.

[2] World Energy Council, "Energy Resources: Solar," *World Energy Counc. 2013 World Energy Resour. Sol.*, pp. 1–28, 2013, [Online]. Available: http://www.worldenergy.org/wp-content/uploads/2013/10/WER_2013_8_Solar_revised.pdf.

[3] S. A. Kalogirou, "Solar thermal collectors and applications," *Prog. Energy Combust. Sci.*, vol. 30, no. 3, pp. 231–295, 2004, doi: 10.1016/j.pecs.2004.02.001.

[4] S. M. Shalaby, A. E. Kabeel, B. M. Moharram, and A. H. Fleafl, "Experimental study of the solar water heater integrated with shell and finned tube latent heat storage system," *J. Energy Storage*, vol. 31, no. March, 2020, doi: 10.1016/j.est.2020.101628.

[5] D. L. Zhao, Y. Li, Y. J. Dai, and R. Z. Wang, "Optimal study of a solar air heating system with pebble bed energy storage," *Energy Convers. Manag.*, vol. 52, no. 6, pp. 2392–2400, 2011, doi: 10.1016/j.enconman.2010.12.041.

[6] A. Gautam and R. P. Saini, "A review on technical , applications and economic aspect of packed bed solar thermal energy storage system," *J. Energy Storage*, vol. 27, no. October 2019, p. 101046, 2020, doi: 10.1016/j.est.2019.101046.

[7] M. Mumtaz, A. Khan, N. I. Ibrahim, I. M. Mahbubul, R. Saidur, and F. A. Al-sulaiman, "Evaluation of solar collector designs with integrated latent heat thermal energy storage : A review," *Sol. Energy*, vol. 166, no. March 2017, pp. 334–350, 2018, doi: 10.1016/j.solener.2018.03.014.

[8] F. S. Javadi, H. S. C. Metselaar, and P. Ganesan, "Performance improvement of solar thermal systems integrated with phase change materials (PCM), a review," vol. 206, no. April, pp. 330–352, 2020.

[9] S. Drissi, T. C. Ling, and K. H. Mo, "Thermal efficiency and durability performances of paraffinic phase change materials with enhanced thermal conductivity – A review," *Thermochim. Acta*, vol. 673, no. November 2018, pp. 198–210, 2019, doi: 10.1016/j.tca.2019.01.020.

[10] M. M. El-Dalatony *et al.*, "Occurrence and characterization of paraffin wax formed in developing wells and pipelines," *Energies*, vol. 12, no. 6, pp. 1–23, 2019, doi: 10.3390/en12060967.

[11] P. Bose and V. A. Amirtham, "A review on thermal conductivity enhancement of paraffinwax as latent heat energy storage material," *Renew. Sustain. Energy Rev.*, vol. 65, pp. 81–100, 2016, doi: 10.1016/j.rser.2016.06.071.

[12] Z. A. K. Zakir Khan, "Experimental investigations of charging / melting cycles of para ffi n in a novel shell and tube with longitudinal fi ns based heat storage design solution for domestic and industrial applications," *Appl. Energy*, vol. 206, no. October, pp. 1158–1168, 2017, doi: 10.1016/j.apenergy.2017.10.043.

[13] H. H. Al-Kayiem and S. C. Lin, "Performance evaluation of a solar water heater integrated with a PCM nanocomposite TES at various inclinations," *Sol. Energy*, vol. 109, no. 1, pp. 82–92, 2014, doi: 10.1016/j.solener.2014.08.021.

[14] M. A. Al-rawaf and J. M. Jalil, "Numerical investigation of thermal performance and phase change of wax paraffin layer surrounding water tank," *Proceeding 15th Sci. Conf.*, no. May 2017, 2016.

[15] A. Shukla, D. Buddhi, and R. L. Sawhney, "Solar water heaters with phase change material thermal energy storage medium: A review," *Renew. Sustain. Energy Rev.*, vol. 13, no. 8, pp. 2119–2125, 2009, doi: 10.1016/j.rser.2009.01.024.

[16] R. Panahi, M. H. Khanjanpour, A. A. Javadi, M. Akrami, M. Rahnama, and M. Ameri, "Analysis of the thermal efficiency of a compound parabolic Integrated Collector Storage solar water heater in Kerman, Iran," *Sustain. Energy Technol. Assessments*, vol. 36, no. October, p. 100564, 2019, doi: 10.1016/j.seta.2019.100564.

[17] S.J. Kline and F.A. McClintock, *Describing Uncertainties in Single-Sample Experiments*, vol. 75 (1). Elsevier B.V., 1953.

[18] S. C. Lin and H. H. Al-Kayiem, "Evaluation of copper nanoparticles - Paraffin wax compositions for solar thermal energy storage," *Sol. Energy*, vol. 132, pp. 267–278, 2016, doi: 10.1016/j.solener.2016.03.004.

[19] M. Mazman, L. F. Cabeza, H. Mehling, M. Nogues, H. Evliya, and H. Ö. Paksoy, "Utilization of phase change materials in solar domestic hot water systems," *Renew. Energy*, vol. 34, no. 6, pp. 1639–1643, 2009, doi: 10.1016/j.renene.2008.10.016.